

The Design and On-sky Results of the Prototype of a Low-Resolution Spectrograph for the Thai National Telescope

Jitsupa Paenoi^{1*}, Christophe Buisset², Kajpanya Suwansukho¹, Wichit Sirichote¹, Piyamas Choochalerm², Suparek Aukkaravittayapun², Griangsak Thummasorn², Surin Ngernsujja², Anuphong Inpun², Pimol Kaewsamoeta², Suchinno Kanthum², Apichat Leckngam², Wayne Orchiston², Krittapas Chaniworawit^{2,3}, Saran Poshyajinda² and Boonrucksar Soonthornthum²

¹Physics Department, Faculty of Science, King Mongkut's Institute of Technology Ladkrabang, Bangkok, Thailand

²National Astronomical Research Institute of Thailand (Public Organization), Chiang Mai, Thailand

³Astronomy Department, University of Florida, Florida, USA

Received: 6 June 2019, Revised: 18 August 2019, Accepted: 3 October 2019

Abstract

The objectives of the research project presented in this paper are to design and develop a Low Resolution Spectrograph for the 2.4 m Thai National Telescope. The Low Resolution Spectrograph will deliver a spectrum in the spectral range (440 -740 nm), with a resolution of R approximately equals to 1,000 at the central wavelength, λ_c , of 600 nm, while observing through a slit with a width of 0.9 arcsecond wide (in long-slit mode) or during slit-less observations. The Low Resolution Spectrograph was designed to have a total weight of less than 20 kg and a maximum displacement due to gravity of less than 6 μm during a 360° rotation of the instrument cube. We have installed a prototype of the Low Resolution Spectrograph on the Thai National Telescope in December 2018. We have tested its performance on stellar objects during a one-night observing run. During these observations, we calibrated the instrument using a Thorium-Argon spectral calibration lamp and a Tungsten lamp and recorded the spectrum of the planetary nebula NGC 2392 in both slit-less and long-slit modes. We measured a spectral resolution of 800-1,300 over the wavelength range 440-740nm, thus demonstrating that the on-sky performance of the prototype was in agreement with the theoretical specifications.

Keywords: low resolution spectrograph, long-slit spectroscopy, slitless spectroscopy, opto-mechanical design, Thai National Telescope
DOI 10.14456/cast.1477.2

1. Introduction

The National Astronomical Research Institute of Thailand (NARIT) and the King Mongkut's Institute of Technology Ladkrabang (KMITL) are currently developing a compact and cost-effective Low-Resolution Spectrograph (LRS) with high throughput for the 2.4 m Thai National Telescope (TNT). This Richey-Crétien telescope is NARIT's main facility for astronomical observations

*Corresponding author: Tel : +66 83-011-2900

E-mail: jitsupapaenoi@gmail.com

in the optical domain. The TNT is located at the Thai National Observatory (TNO), near the summit of Doi Inthanon (latitude of 18.56° N and longitude of 98.46° E), the highest mountain in Thailand (elevation of 2,457m). At this site, the median seeing is 0.9 arcseconds, while the sky brightness is equal to 22.5 and 21.9 magnitude per square arcsecond in the B and V bands, respectively [1]. The TNT is currently equipped with the ULTRASPEC camera, a 4K camera, and a Medium Resolution Spectrograph (MRES). ULTRASPEC is a high-precision photometer that contains a $1k \times 1k$ electron-multiplying CCD with a field of view (FOV) of 7 arcminutes and a plate scale of $0.45''/\text{pixel}$. This instrument is specified to work over the spectral range 330-1,000 nm and has been used to measure rapidly varying phenomena such as transits, flares and outbursts. The 4K camera comprises a cryogenically cooled thin CCD with $4k \times 4k$ pixels. NARIT is currently developing a focal reducer to image a circular FOV of 14 arcminutes on this camera with an image quality close to the seeing limit over the B, V, R and I spectral bands [2]. The Medium Resolution Echelle Spectrograph is a single object fiber-fed medium resolution spectrograph with a spectral resolution close to 15,000 over the spectral band 400- 800 nm. This instrument has been used to measure the spectra of stars down to a limiting magnitude close to 13 and record their radial velocities.

Within this framework, the main objective of the LRS currently being developed at NARIT is to provide spectra of faint point sources (unresolved objects) and extended objects, whose sizes smaller than 3 arcminutes. The spectral resolution of this instrument at the wavelength λ is defined as $R = \delta\lambda/\lambda$ where $\delta\lambda$ is the minimum spectral element that can be resolved by the instrument. The spectral resolution is thus a dimensionless quantity. Our objective is to reach a spectral resolution equal to 1,000 at the wavelength equal to 600 nm. This instrument is design to complete the observing capabilities of the TNT for the following scientific applications: exoplanet detections and atmosphere characterization and the spectroscopic investigation of transit phenomenon.

The second objective of this project is to develop the human capacity to design, manufacture, assemble, align and commission spectrographs in Thailand. Although the optical design of this spectrograph was provided by Professor John Meaburn from the University of Manchester, staff from NARIT and KMITL developed the optomechanical design of the LRS, procured the optical components, manufactured the mechanical parts, and assembled, aligned, and installed the instrument on the TNT. To our knowledge, this is the first time that such a spectrograph has been fully developed and tested in Thailand and our objective is to use this knowledge and the skills acquired during this project to build more spectrographs for astronomical observations, atmospheric studies and space-based remote sensing applications.

Between 2017 and 2019 we developed a prototype of the LRS. Our objectives were to test this prototype on-sky with the TNT, to show that the spectral resolution and field of view of the instrument were in line with specifications and to identify the potential optimizations that will be implemented in the final system.

In this paper, we discuss the specifications of the LRS and present the optical design of the prototype. The mechanical design of the LRS, including the interface with the TNT are described. The results of the Finite Element Analyses are presented to show that the maximum error induced by gravity and thermoelastic effects would be equal to a few μm . The on-sky results obtained in December 2018 during a one-night observing run with the TNT would be reported. The spectrum of the planetary nebula NGC 2392 obtained in long-slit mode over the spectra range of 450-750 nm showing that the spectral resolution, R , was 900 at a wavelength, λ , of 650 nm would be analyzed.

2. Materials and Method

2.1 Specifications and optical design

2.1.1 Specifications

The specifications of the new NARIT Low Resolution Spectrograph (LRS) are presented in Table 1. This spectrograph is specified to deliver a spectrum over the wavelength range of 400-800 nm that covers the visible spectrum and to reach a spectral resolution of R equal to 1,000 at a wavelength equal to 600 nm. The spectrograph provides two observing modes, i.e. the long-slit mode and the slitless mode.

Table 1. Specifications of the Low Resolution Spectrograph developed for the 2.4 m Thai National Telescope.

Parameter	Specification
Spectral domain	400-800 nm
Observing mode	Slitless and Long-slit
Spectral Resolution	$R \approx 1000$ at $\lambda \approx 600$ nm
Slit mechanical length	20 mm
Slit on-sky angular length	3 arcminutes
Slit mechanical width	100 μm
Slit on-sky angular width	0.9''
Dispersion	180 $\text{\AA}/\text{mm}$
Plate scale	37 arcsec/mm
Detector format	2000 \times 500 pixels

The long-slit observations were made by placing the 20 mm slit on the TNT image plane which corresponded to an angular size projected on-sky of 3 arcminutes. This was necessary in order to be able to measure the spectra of (i) extended sources of a few arcminutes, or (ii) two stars (e.g. a science star and a reference star) separated by a few arcminutes.

The slit width, w_s , is equal to 100 μm , which corresponds to an angular size of 0.9 arcseconds. This value is equal to the seeing at the TNO in median conditions [1]. The full spectral domain was then imaged on a detector with a dispersion length, $L_{\text{Dispersion}}$, of 22 mm. The plate scale was specified to be equal to 37 arcsecond/mm and the full 3 arcminutes FOV was imaged along the FOV direction equal to L_{FOV} of 5 mm. The width of the slit image, w_{Slit} , was 23 μm . The dispersion was specified to be equal to 180 $\text{\AA}/\text{mm}$. So, we deduced that the spectral resolution limited by the slit width was 1,500, well above the specified spectral resolution.

The detector was specified to have a pixel size of 10 μm so that the slit image covered 2 pixels, which was close to the Nyquist frequency criterion. Thus, the detector format to cover the specified spectral domain and the specified FOV was equal to 2,000 \times 500 pixels.

2.1.2 Prototype design

Figure 1 shows the side-view of the spectrograph optical design and the left panel in Figure 2 represents the top-view propagation of the beam of light inside the LRS prototype during scientific observations. This prototype was mounted on the TNT which included the rotating mirror M4. The orientation of this mirror was adjusted during the observations to select the instrument mounted on the instrument cube. In the case of observations with the LRS, mirror M2 reflected the beam of light coming from the TNT towards the spectrograph.

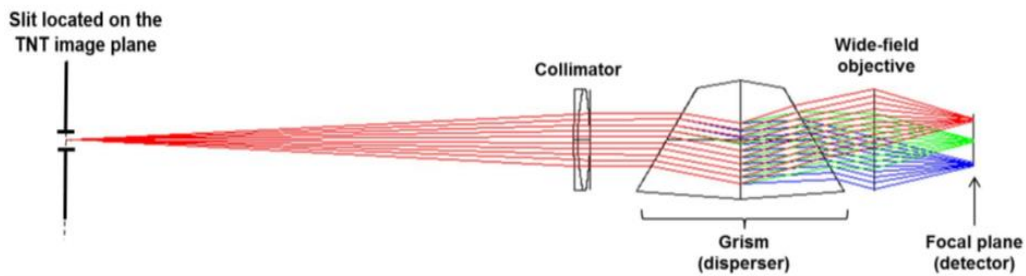


Figure 1. Side-view of the spectrograph optical design [3]

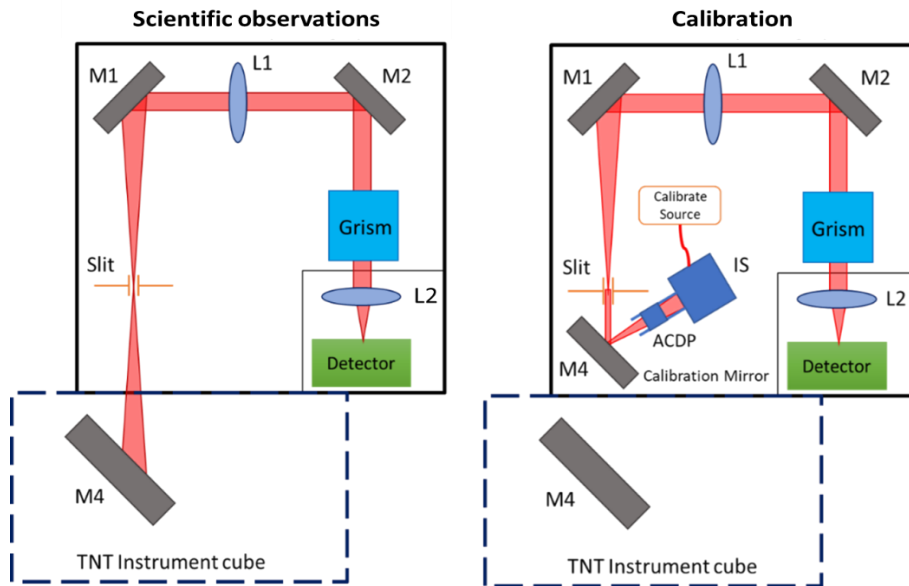


Figure 2. Left-hand panel: Scheme representing the top-view propagation of the light beam inside the spectrograph prototype during the scientific observations. Right-hand panel: Scheme representing the top-view propagation of the light beam inside the spectrograph prototype during the calibration of the instrument

The LRS slit was located in the TNT image plane. The slit selected one linear section of the incident FOV with a length of 3 arcminutes and a width of 0.9 arcseconds. The beam transmitted by the slit was collimated by lens L1 and directed towards the mirrors M1 and M2. These mirrors reflected the beam towards the grism located in the pupil plane. The grism comprised a Volume Phase Holographic (VPH) grating immersed between two prisms. The grism performed the spectral dispersion of the incident beam and transmitted it without any deviation of the central wavelength, λ_c equal to 600 nm. The beam transmitted by the grism was imaged by the lens L2 on the detector.

During the calibration of the spectrograph (Figure 2, right panel), we placed mirror M4 (mounted on a translating stage) in front of the entrance slit. We also injected the light emitted by some flat-field and spectral calibration lamps inside an Integrating Sphere (IS) by using a multi-mode fiber. The IS output face was imaged on the entrance slit via the achromatic doublet ACDP and mirror M4. After reflection by mirror M4, the optical path of the calibration beam emitted by the IS was identical to the optical path of the scientific beam coming from the TNT.

The slit is a 25 mm long 100 μm wide chrome slit, and was manufactured by Ealing. The collimator is a 50.8 mm achromatic doublet with a focal length of 250 mm, made by Thorlabs. This doublet was optimized for the spectral domain 400-700 nm, which is the specified spectral domain of the LRS. The grism was manufactured by Kayser, and the VPH has 930 lines/mm and the angles of the prisms are 30°. The wavelength λ_G not deviated by the grism is equal to 605 nm. The diffraction efficiency is more than 50% over the LRS specified spectral domain, and is more than 90% over the wavelength range of 500-600 nm. The faces of the grisms are coated with an anti-reflective coating that has a reflectivity of less than 1.5% over the specified spectral range of the LRS. The lens L2 is made of one commercial objective manufactured by the company Nikon model Noct-Nikkor AI-s. The focal length of this objective is equal to 58 mm f/1.2, its diameter is equal to 74 mm, and its angle of view is equal to 40.8°.

The detector used in the prototype is a commercial STF-8300 camera manufactured by Diffraction Limited. This camera has a 5.4 μm CCD with 3326 \times 2504 pixels. The dimensions of the detector are thus equal to 18 \times 13 mm², which limits the width of the spectral interval detectable with this prototype to $\Delta\lambda = 330$ nm.

Hence, the results provided by this prototype and presented in Section 3 cover the spectral interval 440-740 nm. This is not compliant with the specified interval for the LRS but has been considered as an acceptable value to verify the behavior of the full instrument and to check that the spectral performance is acceptable.

One advantage of the slitless mode is to be able to observe multiple and fainter targets within a single pointing with the trade-off of coarser spectral resolution, which is highly dependent on the seeing and the size of the object. This mode is suitable for a quick confirmation of objects with broad and prominent spectral features, such as confirming the natures of emission line galaxies or active galactic nuclei, or obtaining the slope of the spectral energy distribution to determine the ages of the underlying stellar populations of galaxies or globular cluster. On the other hand, the long-slit mode provides a constant spectral resolution that is independent of seeing and size of an object. By adjusting the slit width, one can adjust the resolution needed for a specific observation goal.

However, in the long-slit mode, one can only observe up to two objects in a single pointing. This mode is suitable for studying the chemical components, metallicities, and ionization levels of bright objects such as stars and parts of nearby galaxies via their series of absorption and emission features, and for observing the radial motions of binary stars via the doppler shifts of their absorption lines. Thus, the decision to choose between slitless and long-slit modes is based on the scientific goal of each observation program.

2.2 Prototype mechanical design and simulation analyses

2.2.1 Mechanical design

The LRS prototype comprises 24 commercial parts from the Thorlabs catalog and 32 parts that were designed using SolidWorks [4] and manufactured in the NARIT Precision Mechanical Workshop using Computer Numerical Control (CNC) machines.

Figure 3 represents the box of the LRS prototype. This box comprises 8 rectangular panels denoted A, B, C, D, E, F, G and H made of 6061 alloy, the properties of which are described in Table 2.

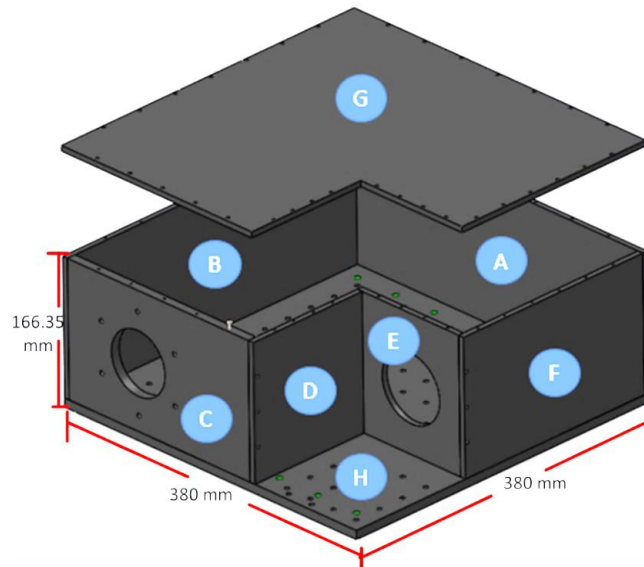


Figure 3. Size of the Low Resolution Spectrograph prototype. Width, length and height are in millimeters. A, B, C, D, E and F are side panels; G is the top panel that covers the spectrograph; and H is the optical bench board

The optical bench H holds the optomechanical components. The side panel components A, B, C, D, E and F are connected to the optical bench H and are covered on the top by the plate G. Panel C has a 70 mm center hole that corresponds to the LRS entrance face placed in front of the TNT instrument cube flange. Panel E has a 70 mm hole where the optical beam from the grism is transmitted to the camera objective (see Figure 4).

The width and the length of the LRS box are both 380 mm and the height is equal to 166.35 mm. The total weight of this structure is equal to 9.99 kg, as shown in Table 2.

Figure 4 represents all the optical and mechanical components of the prototype mounted inside the spectrograph box. Figure 5 shows the SolidWorks model of the prototype mounted on the TNT. Several items have weights lower than 500 g and do not contribute significantly to the total weight of the instrument. The heaviest components are (i) the Grism and the CCD camera with the individual weights of both equal to 0.82 kg; (ii) the Linear Step Motor (LSM) that translates the entrance slits (1.60 kg); and (iii) the adapter of the box for the instrument cube.

Table 2. The mass, size and material type of each panel of the LRS prototype box

Name	Mass (g)	Size (mm)	Material
A	974.89	380 × 150 × 6.35	6061Alloy
B	958.72	373.65 × 150 × 6.35	6061Alloy
C	845.72	245.56 × 150 × 10	6061Alloy
D	361.75	125 × 150 × 6.35	6061Alloy
E	261.55	121.74 × 150 × 6.35	6061Alloy
F	595.41	248.65 × 150 × 6.35	6061Alloy
G	2151.12	380 × 380 × 6.35	6061Alloy
H	3847.07	380 × 380 × 10	6061Alloy
Total	9996.26	380 × 380 × 166.35	6061Alloy

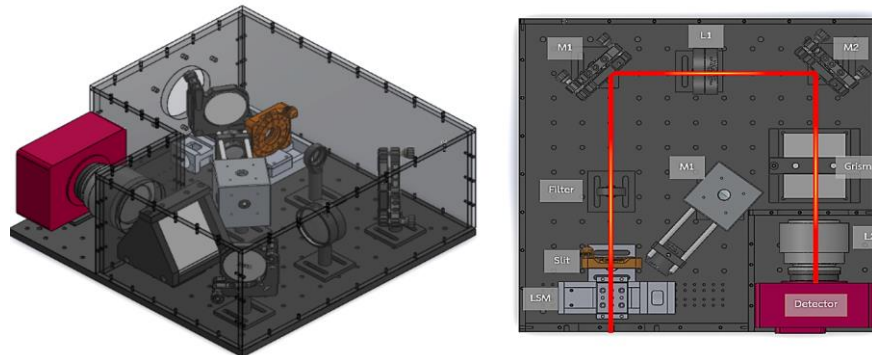


Figure 4. Left-hand panel: Side interior 3D sketch view of the Low Resolution Spectrograph prototype. Right-hand panel: Schematic top-view of the Low Resolution Spectrograph prototype. The red line represents the optical axis of the spectrograph.

The total weight of this prototype is equal to 18.91 kg, which is particularly low for a spectrograph dedicated to a 2 m class telescope. The LRS prototype is thus a light weight and compact instrument. Two advantages of the prototype are that i) it is possible to install the LRS on the TNT and remove it very easily, and ii) the balance of the instrument cube does not need to be adjusted after installing the LRS. It is thus possible to easily install the spectrograph on the TNT for only a few hours of observations and remove it from the instrument cube.

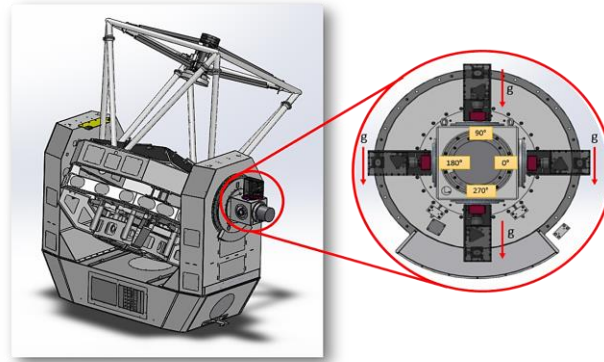


Figure 5. Left-hand panel: 3D view of the Low Resolution Spectrograph prototype mounted on the 2.4 m Thai National Telescope at the Nasmyth focus (SolidWorks model). Right-hand panel: Close-up of the spectrograph mounted on the instrument cube, with the interface between the LRS and the instrument cube shown in purple

2.2.2 Simulation analyses of Finite Element

The Low Resolution spectrograph is mounted on the TNT located inside the dome of the Thai National Observatory. During the night-time, the minimum temperature inside the dome is higher than 0°C while the maximum temperature is lower than 25°C. For these reasons, we decided to perform the thermos-elastic simulations over the temperature range equal to [0°C, 25°C].

During the observations, the Low Resolution Spectrograph rotates slowly around the instrument cube at a maximum angular speed equal to 15°C/h. Thus, we neglect the force due to this rotation and consider gravity to be the only force asserted on the spectrograph.

Figure 6 represents the assumptions used to perform the simulation. We have assumed that the spectrograph is interfaced with the instrument cube via the item “Fixture”. We also assumed that gravity is the only force that is applied to the spectrograph box and to each opto-mechanical component (integrating sphere, collimator, focusing lens). For example, in Figure 6, left-panel, we have represented the direction of gravity for the orientation and the direction of gravity at the orientation is equal to 180°.

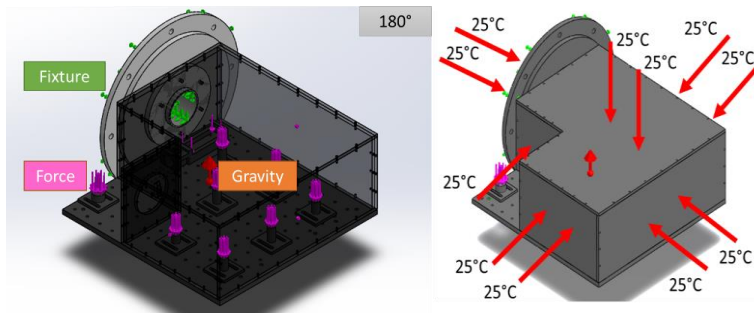


Figure 6. Left-hand panel: Assumptions used for the calculation of the mechanical deformations induced by the gravity of the spectrograph at the orientation equal to 180°. Right-hand panel: Schematic of the assumption made on the environment temperature for the calculation of the deformations induced by the thermos-elastic effect

3. Results and Discussion

3.1 Simulation results

3.1.1 Gravity effect simulation results

During the observations, the orientation of the instrument cube can be fully adjusted between 0° and 360° . This is in order to adjust the orientation of the slit on the observed object and to compensate for the rotation of the field of view. Thus, we performed Finite Element Analyzes (FEA) to simulate the deformations induced by gravity on the LRS box only and to verify that these deformations will not misalign our optical system. These simulations were performed by using the simulation module in the SolidWorks software.

As a first step, we created a mesh element of the LRS prototype. We specified the mesh type to be a standard Solid Mesh, with 4 Jacobian points. The element size was 11.5 mm, with a tolerance of 0.6 mm. With these parameters, we used 492385 nodes and 296275 numbers of elements to model the prototype.

As a second step, we studied the gravitational displacement of the box. For example, in Figure 7 we have represented the deformation of the LRS prototype by assuming that gravity was acting on the base of the prototype box. This corresponds to an orientation θ of the instrument cube equal to 180° .

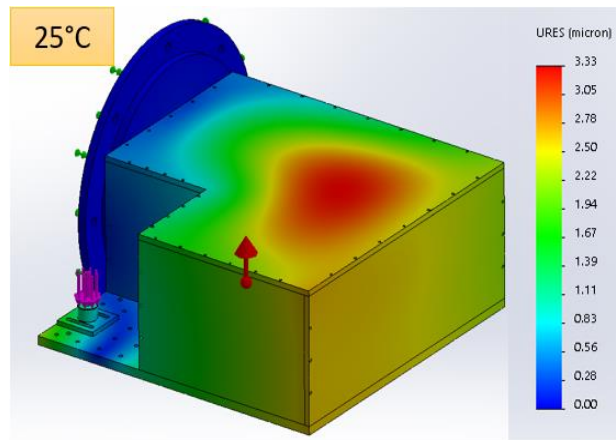


Figure 7. Results of the displacement simulation of the Low Resolution Spectrograph in SolidWorks at the instrument cube orientation θ equal to 180° . The simulation included the following fundamental physical effects: acceleration due to gravity ($|g|$ equal to 9.81 m/s^2), action force with the post, and fixtures in geometry mode.

In this case, we estimated that the maximum displacement value was less than $6 \mu\text{m}$. We repeated these simulations for the following orientations of the instrument cube: θ equal to 0° , 90° , 180° and 270° . We found that the maximum displacement of the box was equal to $3 \mu\text{m}$, which was obtained at θ equal to 180° . In this case, gravity is perpendicular to the optical bench.

We deduced that the maximum deformation of the box during a 360° rotation of the instrument cube is less than $6 \mu\text{m}$. This corresponds to approximately 1 pixel of the camera.

The maximum deformation caused by gravity and simulated using the SolidWorks model is considered acceptable since the prototype will be used to produce spectra during relatively short observing sessions (typically 1 h) that will be compatible with a small variation in the spectrum position on the camera.

3.1.2 Thermal expansion simulation results

We simulated the deformation of the box due to the effect of thermal expansion under the expected range of working temperatures of the Low Resolution Spectrograph (i.e., 0-25°C). This was done by using the SolidWorks model of the of the spectrograph described in the previous Section.

As a first step, we selected the orientation of the instrument cube as θ equal to 270°. At this orientation, gravity is perpendicular to the optical bench. As a second step we calculated the deformation due to both thermal expansion and gravity at a temperature T equal to 0 °C. The results are represented in Figure 7. As a third step, we repeated the simulation at a temperature T equal to 25°C. The results obtained at this temperature are also represented in Figure 7.

We noticed that the deformations in Figures 7 were identical despite the wide change of temperatures, from 0°C to 25°C. Based on these results, we estimated that the deformation of the box due to thermal variations should be less than 1 μm and is therefore negligible.

Thus, we concluded that the LRS prototype design is robust for the typical thermal variations experienced during operational conditions at the TNO. We also concluded that the prototype could be aligned in the laboratory at a temperature close to 20°C and then installed on the TNT without needing any realignment.

3.2 Prototype results obtained during on-sky observations with the TNT

3.2.1 Installation on the TNT and the Observing Procedure

We installed the LRS on the TNT during the engineering night of 22 December 2018. Figure 8 represents the LRS prototype before installation on the TNT (left panel) and after installation on the instrument cube (left-panel). The objectives of this observing run were:

- i) To verify that the full system can be operated in real observing conditions, including calibration of the system, pointing and scientific observations.
- ii) To verify that the performance of the prototype was in line with the specifications under operational conditions. This would be done by measuring the performance on celestial objects during real observations with the TNT.

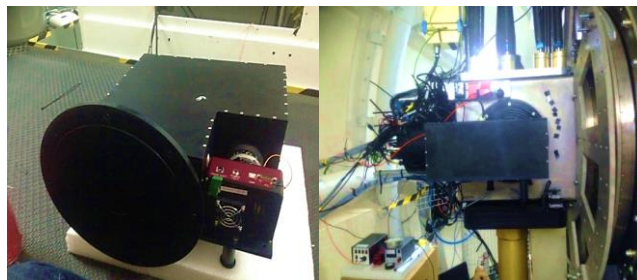


Figure 8. Left-hand panel: The Low Resolution Spectrograph prototype before installation on the TNT. On the left part of the box, there is a large black circular plate that constitutes the interface between the spectrograph and the TNT. Right-hand panel: The LRS prototype mounted on the TNT instrument cube.

It is important to mention that the prototype was aligned at the NARIT Optical Laboratory located in Chiang Mai. We therefore assumed that any misalignment introduced by i) transportation to the TNO, and ii) the pressure and temperature variations between the laboratory and the TNO would only cause a minor variation in the focus.

The procedure for testing the spectrograph involved four steps: focus adjustment; calibration; pointing; and measurement of the spectra. These are now described.

First, we placed the mirror M4 in front of the slit, injected inside the IS the light emitted by a Thorium-Argon spectral calibration lamp, and then recorded the spectrum measured by the detector. This lamp emits light at specific wavelengths and the spectral image comprises several lines, as represented in Figure 9. Each line corresponds to an image of the slit at a given wavelength. The focus adjustment was performed by varying the focus of the wide-field objective L2 and by measuring simultaneously the Full Width at Half-Maximum (FWHM) of the slit image. After adjusting the focus, we measured a FWHM equal to $32.4 \mu\text{m}$ (2 detector pixels) at the wavelength $\lambda = 5740 \text{ \AA}$ that corresponds to a spectral resolution of $R = 1,043$.

Second, we recorded the images of the spectrum provided by the spectrograph while injecting in the IS the light emitted by the Thorium-Argon spectral calibration lamp (Figure 9). We used these images to calculate the relationship between the pixel number and the wavelength by using Isis software [5, 6].

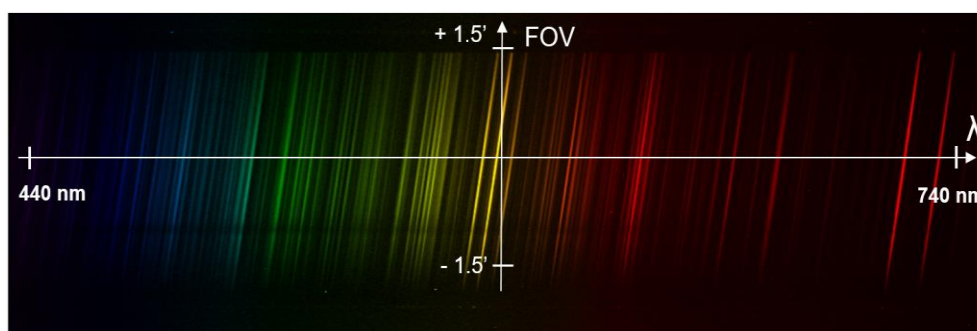


Figure 9. False-color image of the spectrum measured by the spectrograph during the calibration by injecting the light emitted by the Thorium-Argon (ThAr) lamp on the IS. The sloping emission lines correspond to the image of the spectrograph entrance slit at each emission line of the ThAr lamp

Third, we injected the light emitted by a Tungsten lamp inside the IS and we recorded the images of the spectrum provided by the spectrograph. In Figure 10, we noticed that the spectrum measured on the detector fully covers the specified FOV over the spectral interval 440-740 nm. These data confirm the possibility of calculating the spectrograph's instrumental response and pixel-to-pixel variations of the detector response over the FOV and the spectral domain covered by the LRS prototype.

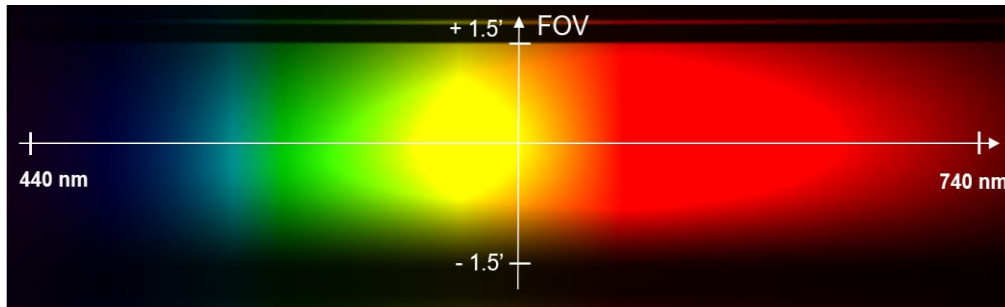


Figure 10. False-color image of the spectrum measured by the spectrograph during the calibration by injecting the light emitted by one tungsten lamp on the IS

The spectrograph response (Figure 11) was calculated as the ratio between the signal detected on the detector and the theoretical spectral irradiance of the source provided by Thorlabs, the supplier of the Tungsten lamp [7]. In Figure 11, we noticed that the normalized response of the spectrograph is more than 0.8 over the spectral interval 500-650 nm and reached a maximum at a wavelength near 560 nm. This is close to the spectral domain 500-600 nm over which the grating diffraction efficiency is maximal. At wavelengths less than 460 nm and more than 720 nm, the response of the instrument was between 0.2 and 0.4 and the limitation was due to the grating efficiency. Over this spectral range the transmission of the spectrograph is very low, and the measurement of the spectrum can be done only on very bright objects.

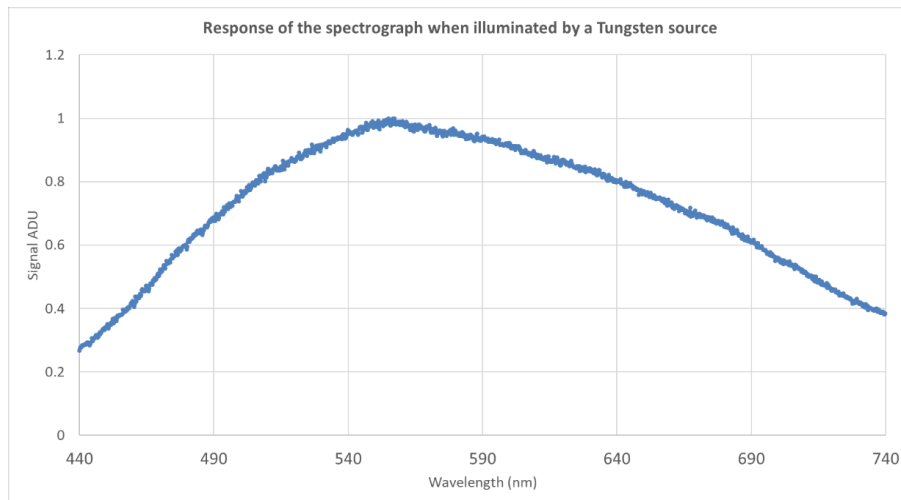


Figure 11. The normalized spectral response of the spectrograph calculated as the ratio between the signal measured on the central line of the detector and the theoretical spectral irradiance of the Tungsten source. The normalization was done to the maximum of the response of the spectrograph.

3.2.2 The Spectrum of NGC 2392

NGC 2392 (the Eskimo Nebula) is a moderately evolved, morphologically complex high-excitation double-shell planetary nebula [1] with a right ascension of 07h 29m10.77 and declination of $+20^{\circ} 54' 42.5''$, and a magnitude of 9.68. Its elevation at the time of the test, between 23:00 and 01:00 local time, varied between $64^{\circ} 10' 59.5''$ and $78^{\circ} 49' 08.3''$.

We selected the Eskimo Nebula to test on-sky the performance of the spectrograph. Indeed, the size of this nebula is equal to 0.47 arcminutes, and making it possible to verify the image quality of the spectrograph over a part of the FOV. This planetary nebula has some specific emissions lines at the wavelengths equal to 486.13 nm, 495.8 nm, 500.7 nm and 656.28 nm, wavelengths which cover the prototype spectral domain. These emission lines were thus used to observe the replica of the nebula and to measure the spectral resolution at these wavelengths.

We used an integration time of 10 seconds for the 4K camera and the LRS in slitless and LRS longslit modes, as illustrated in Figures 12 and 13. We measured the signal-to-noise ratio of NGC 2392 with the 4K camera as 325.2, and for the LRS in longslit mode as 102.317 and in slitless mode as 92. We normalized the spectrum of NGC 2392 and calculated the spectral resolution. For H β it was 801; for OIII 826; for OIII (second line) 845; for HeI 1,097; and for NII 1,224, as illustrated in Figure 14.

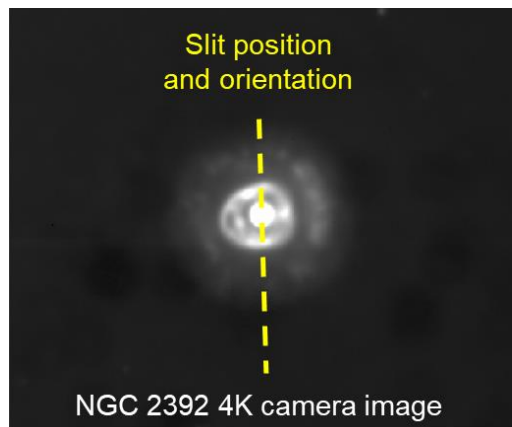


Figure 12. The image of NGC 2392 obtained with the 4K camera mounted on the TNT instrument cube. Integration time equal to 10 s, scale: signal min equal to 8649(0.2) ADU, signal max equal to 45000(1) ADU

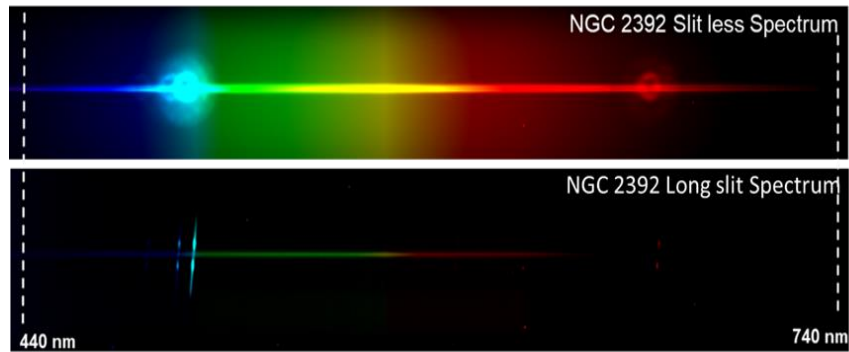


Figure 13. The top panel shows NGC 2392 in slit-less mode. Integration time equal to 10 s, scale: signal min equal to 4537(0.15) ADU, signal max equal to 30000(1) ADU. The bottom-panel shows NGC 2392 in long-slit mode. Integration time equal to 10 s, scale: signal min equal to 1500(0.67) ADU, signal max equal to 2194(1) ADU

We compared the extracted one-dimensional spectrum obtained from the LRS prototype mounted on the Thai National Telescope with one published spectra of NGC-2392 observed with a spectrograph mounted on the 2.16 m Beijing Astronomical Observatory [8] (Figure 14). We noticed in Figure 14 that the location and the shape of the emission lines of the H-alpha, H-beta, NII-doublets, and OII-doublets, as measured with the TNT LRS and as per the already published example, were in good agreement. However, we notice that the continuum measured with the TNT is slightly higher. The potential origins of this difference could be the differences between the calibration method used to process the dataset and the spectral resolution of the spectrographs used to make the observations.

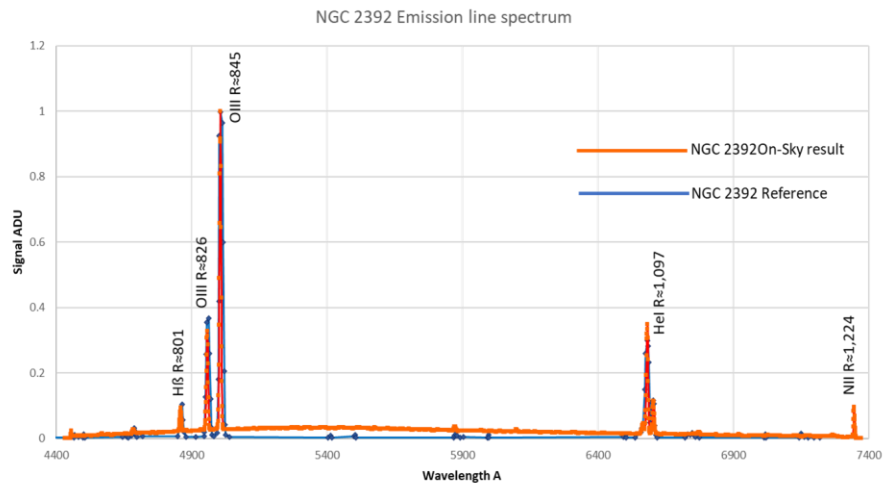


Figure 14. The normalized spectrum of NGC 2392 On-Sky result of LRS prototype for Thai National Telescope (orange curve) compared with published observed spectra of NGC 2392 (blue curve)

4. Conclusions

In this paper, we have presented the design development and on-sky results of the prototype of a Low-Resolution Spectrograph built for the 2.4 m Thai National Telescope. In the next step, we plan to develop a final version of the Low Resolution Spectrograph for the TNT, and build a LRS for the 0.7 m telescope at NARIT's regional observatory at Chachoengsao (Thailand).

References

- [1] Dhillon, V.S., Marsh, T.R., Atkinson, D.C., Bezawada, N., Bours, M.C.P., Copperwheat, C.M., Gamble, T., Hardy, L.K., Hickman, R.D.H., Irawati, P., Ives, D.J., Kerry, P., Leckngam, A., Littlefair, S.P., McLay, S.A., O'Brien, K., Peacocke, P.T., Poshyachinda, S., Richichi, A., Soonthornthum, B. and Vick. A., 2014. ULTRASPEC: a high speed imaging photometer on the 2.4-m Thai National Telescope. *Monthly Notices of the Royal Astronomical Society*, 4009-4021.
- [2] Buisset, C., Deboos, A., Lépine, T., Poshyachinda, S., and Soonthornthum, B., 2016. Design and performance estimate of a focal reducer for the 2.3 m Thai National Telescope. *Optics Express*, 1416-1430.
- [3] Buisset, C., Poshyachinda, S., Soonthornthum, Prasit, B.A., Alagao, M.A., Choochalerm, P., Wanajaroen, W., Lépine, T., Rabbia, Y., Aukkaravittayapun, S., Leckngam, A., Thummasorn, G., S. Ngernsujja, S., Inpan, A., Kaewsamoeta, P., Lhospice, E., Meemon, P., Artsang, P., Suwansukho, K., Sirichote, W. and Paenoi, J., 2018. Activity status and future plans for the Optical Laboratory of the National Astronomical Research Institute of Thailand. *Proceedings of the Third International Conference on Photonics Solutions*, 10714. ICPS2017.SPIE.
- [4] Dassault Systèmes Solidworks Corp., 1997. SolidWorks. USA 25.0.0.5021.
- [5] Nagasawa, D., Marshall, J., DePoy, D., and Mondrik, N., 2014. Conceptual design of a low resolution spectrograph for the Astronomical Observatory of Córdoba. *Ground-based and Airborne Instrumentation for Astronomy V*, SPIE 9147.
- [6] Ammler-von Eiff, M., Sebastian, D., Guenther, E., Stecklum, B. and Cabrera, J., 2015. The power of low-resolution spectroscopy: On the spectral classification of planet candidates in the ground-based CoRoT follow-up. *Astronomische Nachrichten* 336(2), 134-144.
- [7] Shelyak, Ins., 2006. Thorium-Argon bulb. [online] Available at: <https://www.shelyak.com/description-eshel/?lang=en>
- [8] Wu, C., Li, J., Chang, Z., Lin, C., Hu, J. and Ip, W., 2001. Chemical Abundances of the Planetary Nebulae NGC 2392 and NGC 3242. *ASPC*, 246, 339.